Chapter 4

Explore core microbiome diversity in digested versus raw manure impact on lignocellulosic waste composting

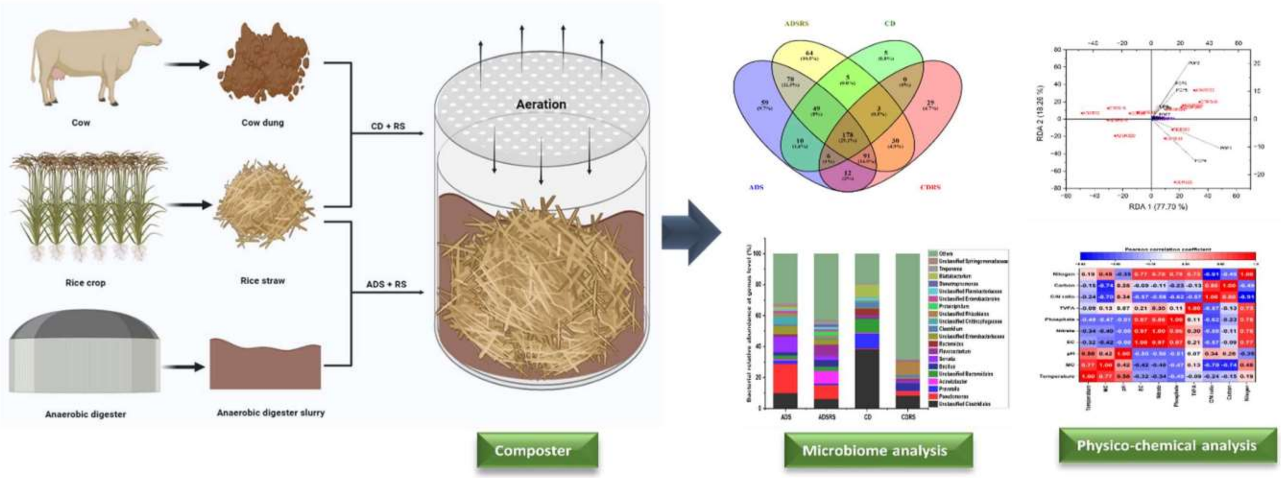

Kushwaha, J., & Dhoble, A. S. (2024). Exploring core microbiome diversity in digested versus raw manure impact on rice straw composting. Environment, Development and Sustainability, 1-22.

4.1 Background

The escalating demand for food, high labor costs, and agricultural shortages, particularly in South and Southeast Asia, had led to the adoption of mechanized combine harvesters for crop harvesting. However, this practice leaves a substantial amount of RS in the fields, which poses challenges due to its low digestibility attributed to high silica and lignin content, rendering it unsuitable for cattle feed. The accumulation of leftover straw necessitates its removal for subsequent crop planting. While open-field burning appears as a convenient solution for farmers, it adversely impacts soil quality by depleting essential nutrients [61]. The substantial amount of leftover digestate (ADS) following digestion also poses a challenge in management, as both ADS and RS contain essential macro elements, including carbon, nitrogen, phosphorus, potassium, and sulfur, alongside inorganic constituents such as Ca, Al, Na, Fe, K, Mg, and Si [49,50]. Composting offers an efficient and effective strategy for managing RS and ADS, mainly attributed to its aerobic conditions that prove more advantageous than anaerobic alternatives [63]. Despite substantial research dedicated to RS, there is still untapped potential in its utilization. Converting RS into compost using ADS as an inoculum offers a promising solution for the agricultural sector. This approach harnesses the valuable outcomes of RS, a lignocellulosic waste, and ADS, addressing their respective challenges in a sustainable manner. The application of advanced technologies, such as green nanotechnology, advanced materials, composites, and nanostructures, enhances composting process efficiency, thereby promoting environmental sustainability and addressing ecological challenges [64,65]. These technologies can accelerate the decomposition of organic matter, enhance microbial activity, and develop more effective composting systems [66,67]. They also contribute to environmental remediation by neutralizing soil contaminants like organic dyes and pollutants [68,69]. Integrating nanotechnology in composting practices can lead to more sustainable approaches by reducing dependence on chemical fertilizers and pesticides, while also optimizing biogas production through anaerobic digestion for renewable energy. Microorganisms play a pivotal role in composting, with previous studies highlighting dominant phyla such as *Firmicutes, Proteobacteria,* and *Bacteroidetes* [70]. These phyla are renowned for their efficient decomposition of complex organic materials, including hemicellulose, cellulose, lignin, xylan, and chitin. In addition to this, specific species like *Bacillus, Acinetobacter, Luteimonas, Pseudomonas,* and *Stenotrophomonas* have demonstrated a remarkable ability to fix nitrogen and solubilize phosphate, contributing to enhanced plant growth [69,70]. Their collective activities contribute to transforming organic waste into nutrient-rich compost, facilitating sustainable agricultural practices [60,61] .This study aims to investigate the effects of ADS and raw cattle manure (CD) on RS, to scientifically compare these treatments and elucidate the core microbiomes and their associated physicochemical properties. The research seeks to understand the interactions between microbial community dynamics and physicochemical parameters, such as temperature, pH, moisture content, and nutrient composition, during the composting of RS. The hypothesis posits that integrating specific process parameters, such as aeration, carbon-to-nitrogen ratio, and moisture management, with microbial dynamics can yield valuable insights into the efficient biodegradation of RS and the effective utilization of ADS in compost production. The investigation analyzed the transformations of RS during composting using advanced techniques such as Fourier Transform Infrared Spectroscopy (FTIR) and Scanning Electron Microscopy (SEM). FTIR was employed to identify and characterize the chemical bonds and functional groups present in the RS, while SEM provided detailed images of the RS's surface morphology, revealing structural changes over time. The study also examined shifts in the microbiome using 16S rRNA metagenomic sequencing to compare the microbial communities at the beginning and end of the composting process from two different inoculum sources. This sequencing technique enabled a detailed analysis of bacterial and archaeal populations, shedding light on microbial succession and functional dynamics. Additionally, the investigation evaluated changes in lignocellulosic components—lignin, cellulose, hemicellulose, and silica content—within the RS. By integrating these analytical methods, the study provided comprehensive insights into the efficacy of composting processes, microbial dynamics, and the stability of composting systems under various process parameters. This detailed approach enhances the understanding of microbial interactions and physicochemical transformations, contributing to the optimization of composting practices. Integrating ADS and RS into composting processes demands a balanced approach to optimize benefits and mitigate negative effects. Effective management of ADS and RS necessitates understanding their nutrient profiles and impacts on soil health to develop sustainable utilization and disposal strategies. Properly managed, their combined use can enhance soil fertility and structure, promoting sustainable agricultural practices.

4.1.1 Experimental design and setup

The study employed in these vessels: Maintained a 5:2 CD: RS ratio, while the other replaced CD with ADS [8]. ADSRS denoted anaerobically digested manure with RS, while CDRS represented raw manure with RS. Compost moisture content was adjusted to 65% by incorporating deionized water. The mixture was turned every two days using a forklift during the 60-day cycle, and samples weighing 10 g were collected every five days from distinct sections.

4.1.2 Raw material

Fresh ADS was acquired from a nearby biogas facility at coordinates 25° 11' 33.95" N and 82° 51' 19.06" E in Varanasi, India. RS was reaped at the close of the growing season from an agricultural plot at Banaras Hindu University (BHU), Varanasi, Uttar Pradesh, India, in November 2022. Following the harvest, the RS underwent mechanical fragmentation using an electric fodder-cutting machine to create smaller segments. It was immediately transported to the laboratory, stored in zip-lock bags, and kept at room temperature. The RS experienced a two-step desiccation process to reduce moisture content. Initially, it was naturally air-dried to eliminate surplus moisture, and subsequently, it was subjected to drying at 50°C in a hot air oven (Equitron, Stream Series) until reaching a consistent weight. Afterward, the RS was further processed into smaller sizes (2 - 3 cm) using an electric grinder (Philips Supreme 550W). The characteristics of the raw material and inoculum are shown in Table 4.1.

Table 4.1. Characteristics of inoculum and raw material

Characteristics*	**Rice straw (RS)**	**Anaerobic Digester Slurry (ADS)**	**Cow Dung (CD)**
Total Solids (TS, %wt)	92.6 1 ± 0.19	7.26 ± 0.88	18.5 ± 0.40
Volatile Solids (VS, %wt)	82.10 ± 0.38	4.59 ± 0.26	14.90 ± 0.62
VS/TS	0.90 ± 0.22	0.60 ± 0.12	0.79 ± 0.96
Moisture content (%)	6.53 ± 0.19	92.94 ± 0.86	81.69 ± 0.72

*Numbers are mean ± standard deviation from three replicates

4.2 Results and Discussion

4.2.1 Physicochemical analysis

Raw RS contained 42.9% cellulose, 36.86% hemicellulose, and 8.62% lignin, all of which were crucial for microbial breakdown, making it a valuable substrate for bioenergy processes. However, the high silica content (45.98% of ash) in RS posed processing challenges, as silica was non-biodegradable. In terms of carbon content, RS (41.68%), anaerobic digester slurry (29.39%), and CD (43.12%) showed varying levels, with CD having the highest potential for energy recovery. Hydrogen levels were quite similar across the materials, ranging from 5.59% in ADS to 6.89% in RS. In comparison, nitrogen content remained below 1% for all three materials, suggesting the potential need for nitrogen supplementation to enhance microbial processes. During the composting process, the ADSRS temperature started at 28.67°C, the CDRS temperature at 29.1°C, and the ambient temperature at 19°C on Day 0, represented in

Figure 4.1. (a). Subsequently, the ADSRS temperature increased significantly, peaking at 53.39°C on Day 5, signifying intense microbial activity and rapid decomposition [75]. After Day 5, the ADSRS temperature gradually declined, while the CDRS temperature slightly rose, indicating a transition to the cooling down and ripening stage as microbial activity subsided. Fluctuations in ambient temperature throughout the process could influence overall temperature trends [76]. By Day 60, ADSRS and CDRS temperatures decreased, remaining close to each other, indicative of a stable and mature compost ready for use as a nutrient-rich soil amendment. Throughout the composting process, pH in both ADSRS and CDRS showed fluctuations in *Figure 4.1. (b)* but consistently maintained a slightly alkaline range, starting at 7.8 and 7.26, respectively, on Day 0.

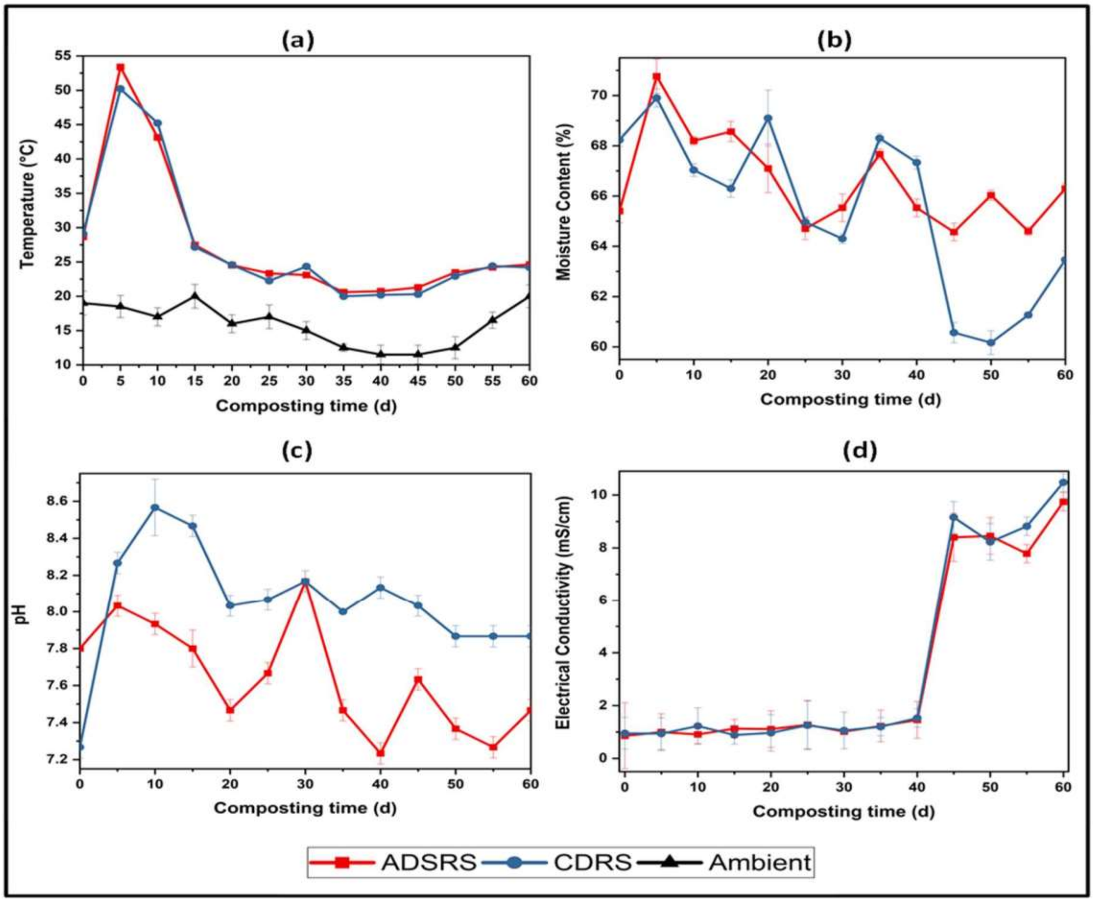

Figure 4.1. (a) Temperature, (b) Moisture Content, (c) pH, (d) Electrical conductivity in composting of rice straw (RS) with cow dung (CD) and anaerobic digester slurry (ADS)

This pH environment was favorable for microbial activity and decomposition [65]. As the composting process progressed, the pH stabilized around 7.46 in the ADSRS and 7.86 in the CDRS by Day 60, indicating a neutral to slightly alkaline environment that fostered nutrient availability and overall compost stability. The pH initially showed an increase followed by a decrease, possibly influenced by microbial activity and the decomposition of organic matter [75]. In *Figure 4.1. (c)*, moisture content levels in both exhibited dynamic changes. At Day 0, moisture content started at 65.4 % in ADSRS and 68.23 % in CDRS, indicating a moderate to high moisture level in the compost [77]. As the days progressed, the moisture content fluctuated, showing variations in the water content as the compost matured. By Day 60, the moisture content stabilized at approximately 66.3 % in ADSRS and 63.46 % in CDRS, reflecting a relatively balanced and optimal composting moisture level [71]. In *Figure 4.1. (d)*, at Day 0, electrical conductivity levels were low, measuring 0.85 mS/cm in the ADSRS and 0.95 mS/cm in the CDRS, indicating a relatively low concentration of dissolved ions in the compost. As days progressed, the electrical conductivity in both stages fluctuated, reflecting variations in ion concentration [72,80]. By Day 60, the electrical conductivity had stabilized at higher levels, around 9.74 mS/cm in the ADSRS and 10.47 mS/cm in the CDRS, suggesting an increased dissolved ion concentration as the compost matured [52].

During the composting process, in *Figure 4.2. (a)*, ADSRS nitrate levels commenced at a moderate level of 13.58 mg/kg, gradually increased, peaked at day 50 (361.56 mg/kg), and slightly decreased after that. In contrast, the CDRS condition began with higher nitrate levels 20.72 mg/kg, displayed fluctuations, peaked at day 55 (267.95 mg/kg), and then underwent a subsequent decline. Whereas phosphate concentration is in *Figure 4.2. (b)* levels varied, starting at 3.75 mg/kg in the ADSRS and 2.35 mg/kg in the CDRS on Day 0. By Day 60, the phosphate concentration had stabilized at higher levels, approximately 28.16 mg/kg in the ADSRS and 26.75 mg/kg in the CDRS. The observed patterns in nitrate and phosphate levels for both ADSRS and CDRS conditions showcase unique trajectories, emphasizing the diverse microbial activities and nutrient transformations occurring in distinct composting scenarios [67]. In *Figure 4.2. (c)* ADSRS, total volatile fatty acid (TVFA) levels started at 1594.21 mg/kg on day 0, exhibited fluctuations, and spiked up at 11007.61 mg/kg on day 15, possibly due to an increase in microbial activity such as *Proteobacteria, Firmicutes, Bacteroidetes,* and *Actinobacteria* [58,81]. Conversely, CDRS began at a lower value of 607.32 mg/kg, rapidly increased to 3340.24 mg/kg by day 10, fluctuated, and stabilized around days 25 to 35, followed by a decline. These fluctuations and trends reflected the intricate interplay of microbial activity and organic matter decomposition, shedding light on the dynamic nature of composting processes [107]. At the start, ADSRS and CDRS both showed C/N ratios of 40.00 and 38.91, respectively. After 60 days, ADSRS and CDRS exhibited stabilized C/N ratios around 12, suggesting compost stability [74]. This value indicated a C/N ratio similar to stable soil organic matter humic substances, signifying potential compost maturity [74,101]. Initially, both conditions displayed carbon percentages of 40.00 (ADSR) and 38.91 (CDRS) on day 0. As the composting process progressed, ADSRS and CDRS experienced fluctuations in carbon percentage. On day 10, ADSRS had a carbon percentage of 28.16 %, while CDRS had 32.52 %. Over the following days, the carbon percentages continued to vary, with ADSRS recording 30.17 % and CDRS showing 27.07 % on day 60. At day 0, both ADSRS and CDRS conditions started with a nitrogen percentage of 1 %. As the composting process unfolded, notable changes occurred. By day 10, the nitrogen percentage increased to 1.90 % for ADSRS and 1.57 % for CDRS [78]. Subsequently, on day 20, the nitrogen percentage values were 1.67 for ADSRS and 1 for CDRS. On days 30 and 40, the values stabilized at 1 for both conditions. An interesting shift occurred on day 50, with values rising to 2.52 % for ADSRS and 2.29 % for CDRS. This trend continued on day 60, with nitrogen of 2.16 % for ADSRS and 2.51 % for

CDRS. These fluctuations in nitrogen content provided insights into the dynamic changes that occurred during the composting process under different conditions [75].

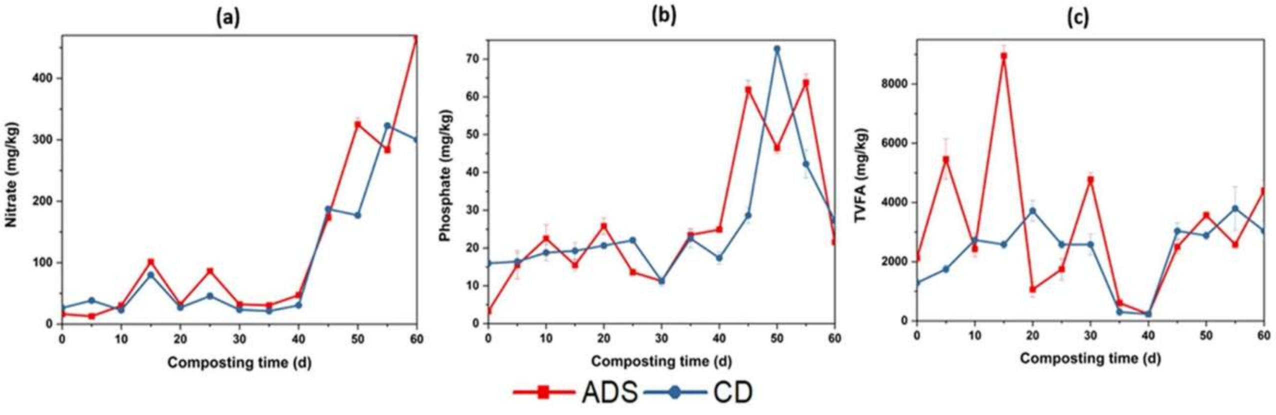

Figure 4.2. (a) Nitrate (b) Phosphate (c) Total Volatile Fatty Acids (TVFAs) in composting of rice straw (RS) with cow dung (CD) and anaerobic digester slurry (ADS)

In *Figure 4.3. (a)*, Pearson correlations reveal relationships in ADSRS composting. pH correlates positively with TVFA and carbon and negatively with electrical conductivity and nitrogen [76]. Nitrate, phosphate, and electrical conductivity positively correlate [76]. In *Figure 4.3. (b)*, Pearson correlations outline CDRS composting. Nitrate, phosphate, and electrical conductivity demonstrate positive connections, and the p-value was less than 0.05. TVFA relates positively to pH and temperature, while carbon and nitrogen exhibit a positive correlation, as stated by [88]. These correlations elucidate the interplay of temperature, moisture, pH, and nutrient dynamics during composting, enhancing comprehension of microbial processes and nutrient transformations.

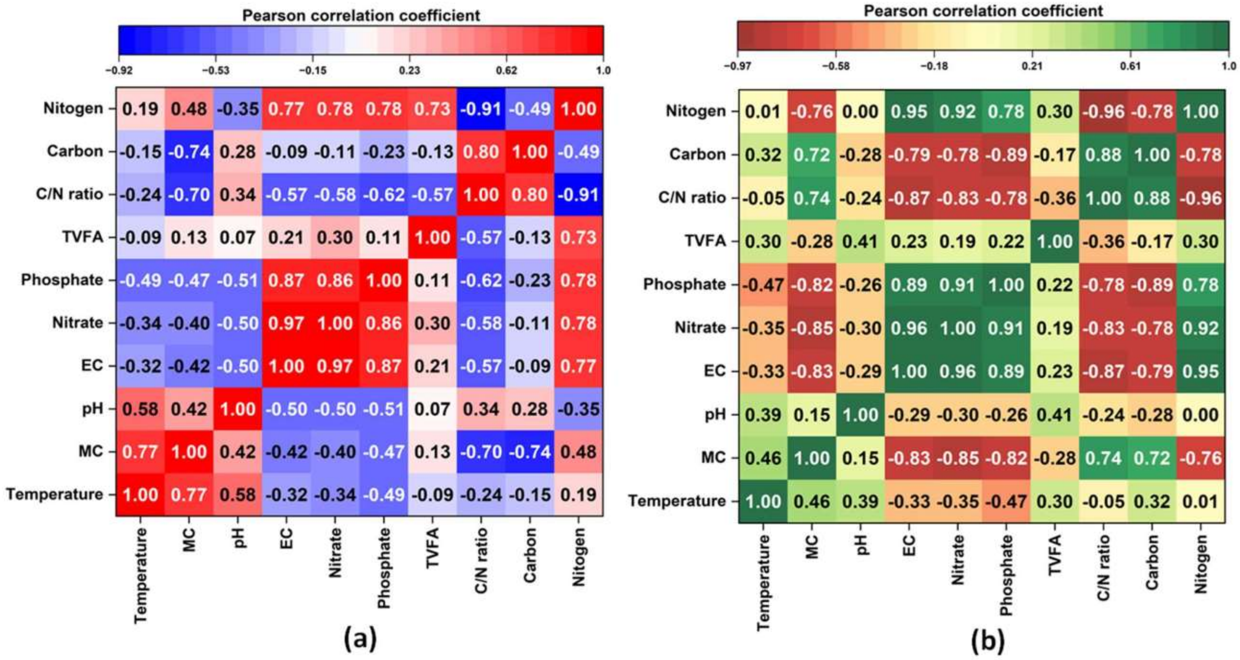

(a)

	Temperature	MC	pH	EC	Nitrate	Phosphate	TVFA	C/N ratio	Carbon	Nitogen
Nitogen	0.19	0.48	-0.35	0.77	0.78	0.78	0.73	-0.91	-0.49	1.00
Carbon	-0.15	-0.74	0.28	-0.09	-0.11	-0.23	-0.13	0.80	1.00	-0.49
C/N ratio	-0.24	-0.70	0.34	-0.57	-0.58	-0.62	-0.57	1.00	0.80	-0.91
TVFA	-0.09	0.13	0.07	0.21	0.30	0.11	1.00	-0.57	-0.13	0.73
Phosphate	-0.49	-0.47	-0.51	0.87	0.86	1.00	0.11	-0.62	-0.23	0.78
Nitrate	-0.34	-0.40	-0.50	0.97	1.00	0.86	0.30	-0.58	-0.11	0.78
EC	-0.32	-0.42	-0.50	1.00	0.97	0.87	0.21	-0.57	-0.09	0.77
pH	0.58	0.42	1.00	-0.50	-0.50	-0.51	0.07	0.34	0.28	-0.35
MC	0.77	1.00	0.42	-0.42	-0.40	-0.47	0.13	-0.70	-0.74	0.48
Temperature	1.00	0.77	0.58	-0.32	-0.34	-0.49	-0.09	-0.24	-0.15	0.19

(b)

	Temperature	MC	pH	EC	Nitrate	Phosphate	TVFA	C/N ratio	Carbon	Nitogen
Nitogen	0.01	-0.76	0.00	0.95	0.92	0.78	0.30	-0.96	-0.78	1.00
Carbon	0.32	0.72	-0.28	-0.79	-0.78	-0.89	-0.17	0.88	1.00	-0.78
C/N ratio	-0.05	0.74	-0.24	-0.87	-0.83	-0.78	-0.36	1.00	0.88	-0.96
TVFA	0.30	-0.28	0.41	0.23	0.19	0.22	1.00	-0.36	-0.17	0.30
Phosphate	-0.47	-0.82	-0.26	0.89	0.91	1.00	0.22	-0.78	-0.89	0.78
Nitrate	-0.35	-0.85	-0.30	0.96	1.00	0.91	0.19	-0.83	-0.78	0.92
EC	-0.33	-0.83	-0.29	1.00	0.96	0.89	0.23	-0.87	-0.79	0.95
pH	0.39	0.15	1.00	-0.29	-0.30	-0.26	0.41	-0.24	-0.28	0.00
MC	0.46	1.00	0.15	-0.83	-0.85	-0.82	-0.28	0.74	0.72	-0.76
Temperature	1.00	0.46	0.39	-0.33	-0.35	-0.47	0.30	-0.05	0.32	0.01

Figure 4.3. Pearson correlation analysis of physiochemical properties (a) anaerobic digester slurry (ADS), (b) cow dung (CD)

4.2.2 Alterations in the chemical composition and physical structure of rice straw

The FTIR analysis assessed the impact of inoculum on the chemical composition and structure of composted RS, focusing on the 4000-400 cm^{-1} range. Comparative assessments were conducted among the FTIR spectra of ADSD0, CDD0, ADSD60, and CDD60, as shown in *Figure 4.5.* The appearance of a peak at 1527 cm^{-1} signifies the potential presence of a benzene ring, potentially resulting from a reduction in lignin content during the composting process [79]. The distinct peaks observed at 1394 cm^{-1} correspond to cellulosic biomass in the samples, indicating exposed cellulose availability after composting [80]. In all four samples, notable variations in peak heights at 1118 cm^{-1} indicate changes in the C-N and C-H bonds of aliphatic amines and alkyl halides [84]. The two measured peaks at 2927 cm^{-1} represent C-H methyl and aliphatic methylene groups. Microbial oxidation of aliphatic and peptide carbon chains reflected in these bands, specific to C-H aliphatic molecules, and their intensity diminishes with co-composting [84]. The asymmetry of the bands indicates the presence of OH and NH groups around 3426 cm^{-1} [88].

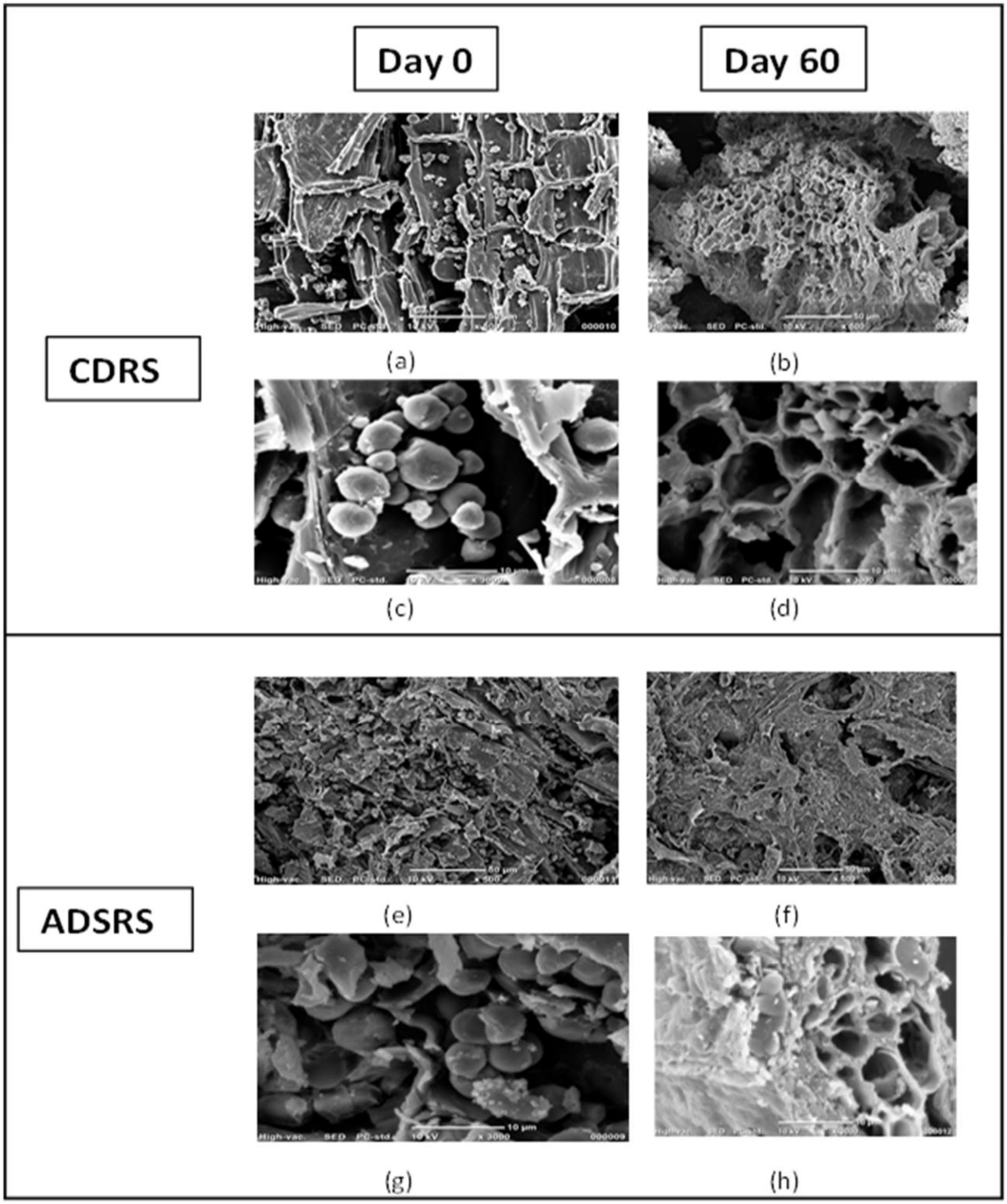

Figure 4.4. Images of SEM micrographs of rice straw (RS) compost at day 0 (a, c) and day 60 (b, d) with cow dung (CD) at 50X and 10X, and rice straw (RS) at day 0 (e, g) and day 60 (f, h) with anaerobic digestate slurry (ADS) at 50X and 10X

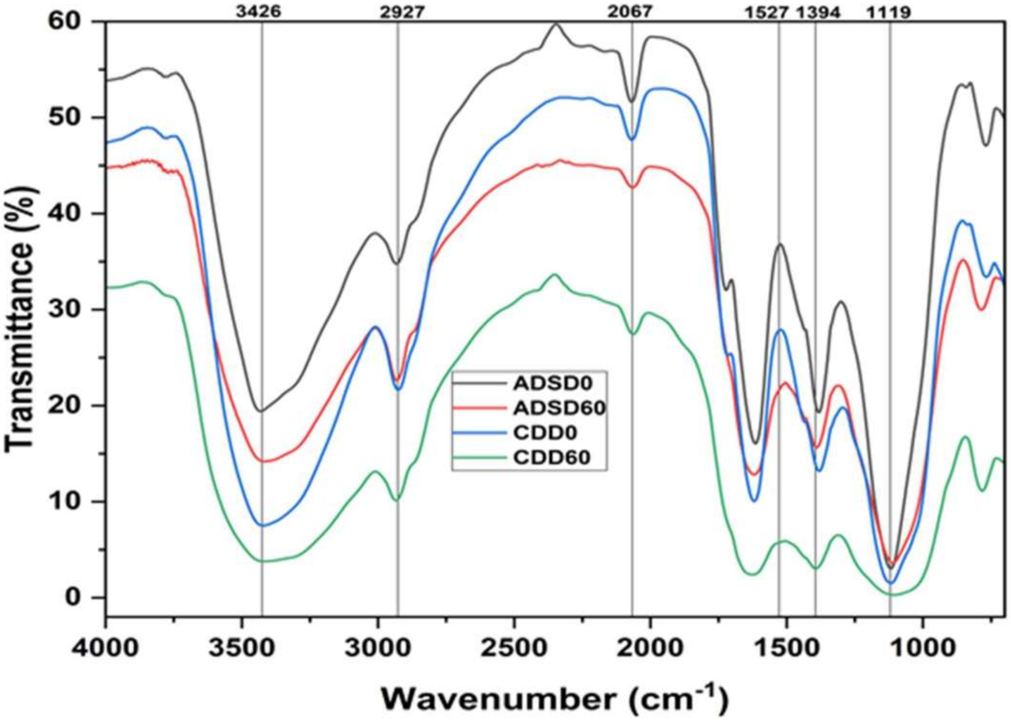

Figure 4.5. FTIR spectra of ADSD0 (day 0), ADSD60 (day 60), CDD0 (day 0), and CDD60 (day 60)

Scanning Electron Microscopy (SEM) images of RS compost were captured at day 0 as shown in *Figure 4.4.* (a, c, e, and f) and day 60 (b, d, f, and h) for CD and ADS at 50X and 10X. The SEM images of RS samples reveal notable characteristics such as intricate ridges, grooves, and well-organized fibrils [87]. Notably, after 60 days, visible pore spaces were observed in both CD and ADS, which are almost similar. when viewed at 50X and 10X magnifications. Remarkably, after 60 days, distinct pore spaces became evident in both CD and ADS samples, possibly indicating heightened microbial activity while exhibiting similarity at 50X and 10X magnifications.

4.2.3 Flow cytometry analysis of microbial population

Autocorrelation analysis, utilizing data from consecutive days (time points 1 to 6), has yielded valuable insights into microbial populations' continuous and dynamically evolving behaviour and the influence of perturbations, as shown in *Figure 4.6.* In this context, "delay" indicates the temporal gap between a given day's dataset and the lagged values derived from previous days. The employment of a 10-day delay involves comparing the data from a specific day (such as D1) with the data from the immediately preceding day (such as D0), aiming to uncover noticeable patterns or dependencies that existed between successive days. Distance matrix computations were employed in identifying microbial succession patterns, and autocorrelation analysis revealed shifts and temporal interdependencies within microbial populations [88]. Furthermore, the extremum in distance measurements has been utilized to gauge the stability of phenotypes [57]. ADS showed delays 2, 3, and 6, which exhibited comparable dynamics characterized by ongoing perturbations and consistent dissimilarity values. These findings suggest that no substantial changes are evident based on differences calculated using the Root Mean Square Deviation (RMSD).

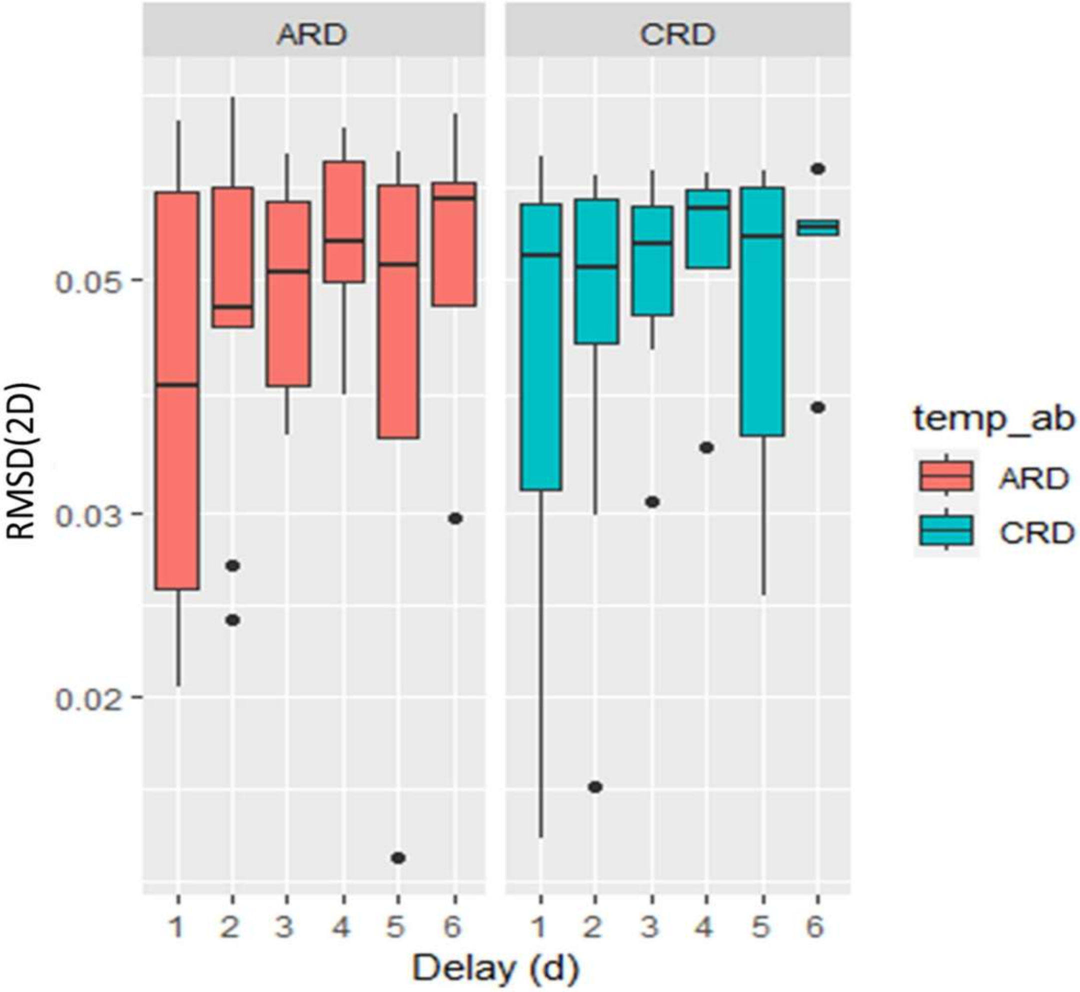

Figure 4.6. Autocorrelation plot for dissimilarity RMSD (2D) vs Delay.

Meanwhile, persistent alterations in the distances related to Forward Scatter (FSC-A) and Side Scatter (SSC-A) have provided a clear picture of the evolving microbial dynamics. In the context of the CD analysis, dynamic changes have come to the forefront. There is a similarity in the differences observed at delays 1 and 5. In contrast, delays 2, 3, and 4 have exhibited linear changes. Notably, delay 6 has witnessed a pronounced spike in the CD analysis, revealing a substantially different perturbation dynamic. This disparity indicates substantial alterations within the microbial community structure and behavior.

4.2.4 Hierarchical clustering of the bacterial and archaeal community

Figure 4.7 (a) displays the relative abundance of various bacterial taxa in the initial composting sample (ADS and CD) and final (ADSRS and CDRS). The composting microbial community exhibited diversity, encompassing various bacterial taxa that played roles in the decomposition and breakdown of organic materials. Within the ADS sample, *Pseudomonas* constituted 18.93% and Bacillus 10%. The ADSRS sample displayed dominance of Others at 42.7% and *Flavobacterium* at 6.96%. In contrast, the CD sample demonstrated *Unclassified Clostridiales* at 38.16% and *Unclassified Bacteroidales* at 9.15% as prevailing taxa. Similarly, in the CDRS sample, Others accounted for 68.37%, and *Unclassified Chitinophagaceae* for 8.47% as dominant taxa. *Clostridiales, Bacillus,* and *Clostridium* are known for their involvement in the breakdown of complex organic matter and the production of various enzymes that degrade organic compounds [86]. *Pseudomonas* is often associated with the degradation of complex organic compounds, including hydrocarbons and lignin [109]. *Prevotella* and *Proteiniphilum* may play roles in the decomposition of proteins and nitrogen-containing compounds [88]. *Bacteroides* and *Unclassified Bacteroidales* are known for their roles in the degradation of carbohydrates, lignin, and complex polysaccharides [60]. The ADSRS sample has a higher abundance of *Flavobacterium, Unclassified Rhizobiales,* and *Unclassified Flavobacteriaceae than* the other samples. The CD sample has a significantly higher abundance of *Unclassified*

Clostridiales and *Unclassified Bacteroidales,* which substantially degraded intricate carbohydrates and lignocellulosic substances [89].

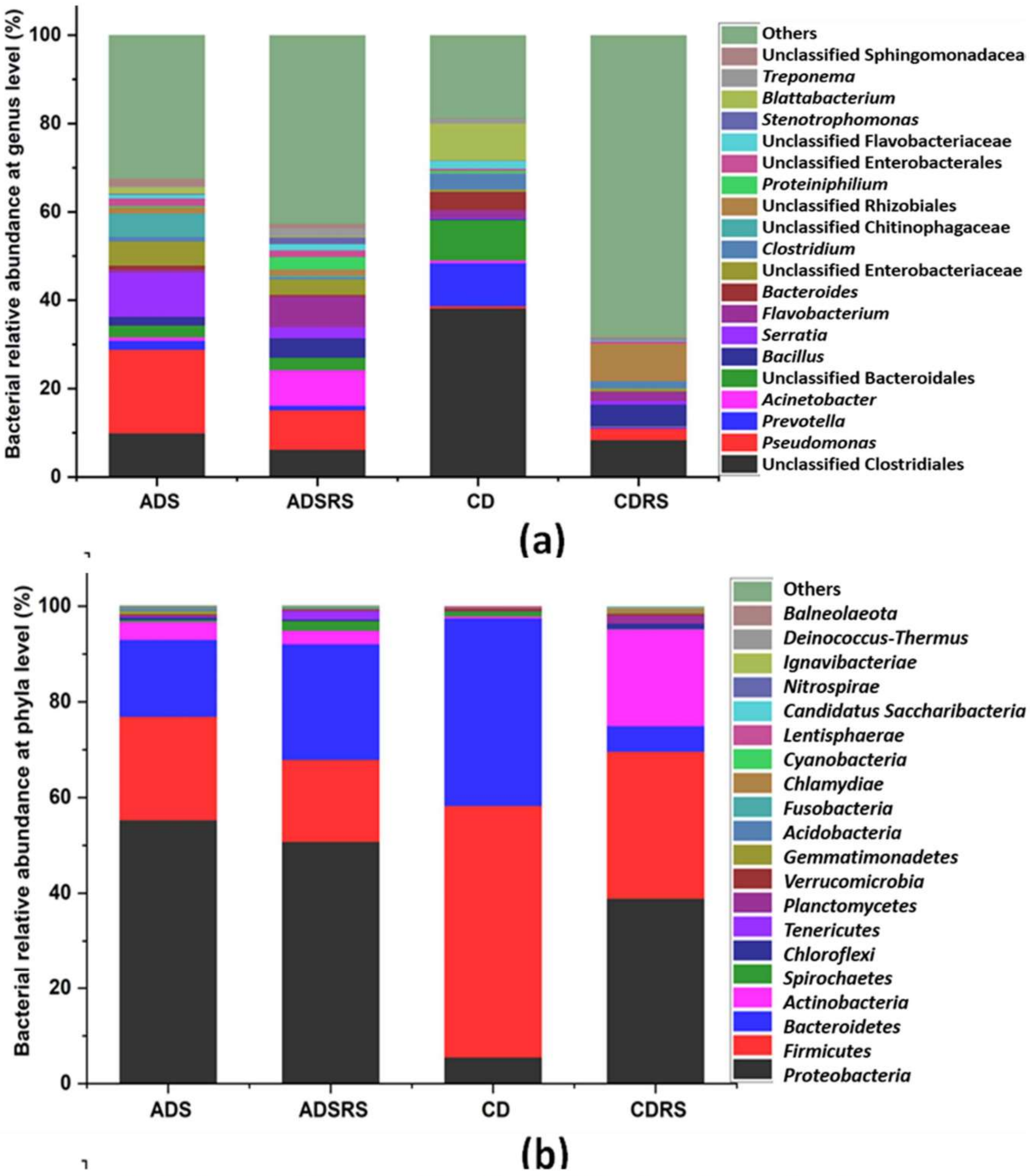

Figure 4.7. Analysis investigated the composition of bacterial abundance at genera level (a), phyla level (b), specifically the top 20 genera, before and after composting rice straw with cow dung (CDRS) and anaerobic digester slurry (ADSRS) as inoculum, compared to raw inoculum samples CD and ADS.

In *Figure 4.7. (b)*, the data illustrates the varying prevalence of bacterial phyla across distinct composting. During the initial ADS, *Proteobacteria* (55.27%) take the lead, implying a high activity level in organic matter breakdown. As composting progresses in the ADRS mature, *Bacteroidetes* (24.19%) and *Firmicutes* (17.16 %) gain prominence, accompanied by *Actinobacteria* (2.80%) and *Spirochaetes* (2.01%), indicating dynamic shifts in microbial communities. In the CD scenario, *Firmicutes* (52.78%) dominate, signifying advanced decomposition, while CDRS displays *Actinobacteria* (20.21%) and *Firmicutes* (30.70%) as primary contributors, suggestive of a mature composting process. The prevalence of *Proteobacteria* and *Firmicutes* stands out prominently, attributed to their adaptable metabolic capabilities and prowess in decomposing a wide range of organic substrates [58, 60]. Additionally, *Bacteroidetes* and *Actinobacteria* significantly contribute to the degradation of intricate carbohydrates and lignocellulosic materials [92]. In ADS, the dominant archaeal taxa include *Unclassified Haloarcula* (23.17 %), *Unclassified Haloferax* (15.77 %), and *Unclassified Haloarcula* (14.81 %). Conversely, in the ADSRS sample, *Methanomassiliicoccus* (22.77 %), *Halonotius* (36.46 %), and *Methanonatronarchaeaceae* (11.31%) were the dominant taxa. This trend continues in the CD sample, with *Methanothrix* (31.37%), *Unclassified Methanobrevibacter* (13.73 %), and *Natrinema* (15.36 %) as the dominant taxa. In the CDRS sample, the dominant taxa consist of Others (49.12 %), *Unclassified Methanobrevibacter* (17.54 %), and *Unclassified Halorubrum* (5.26 %). *Haloarchaeobius, Haloferax, Halonotius,* and *Halobium* detected in both the inoculum CD and ADS samples are believed to have played a role in the decomposition of organic matter, particularly within the high-salt conditions of CD composter [90]. The relative abundance of archaeal taxa varies among the samples, indicating differences in their archaeal community composition. This variability may reflect the diversity of habitats, environmental conditions, and organic substrates in each composting sample.

4.2.5 Microbial comparative analysis

4.2.5.1 Core microbiome

Prevalence values assigned to various microbial taxa in the core microbiome reflect their abundance and occurrence during composting. Specific taxa, indicated in *Figure 4.8* by a prevalence value of 1, consistently populate the core microbiome, including *Unclassified_Rhizobiales*, *Unclassified_Enterobacteriaceae*, *Serratia*, *Bacillus*, *Unclassified_Bacteroidales*, *Pseudomonas*, and *Unclassified_Clostridiales*, among others. These microbes play pivotal roles in organic matter decomposition, nutrient cycling, and the overall functioning of the composting system. Microorganisms with lower prevalence values may also inhabit the core microbiome, albeit with lesser abundance or occurrence, contributing to specific functions within the composting system, albeit to a reduced extent.

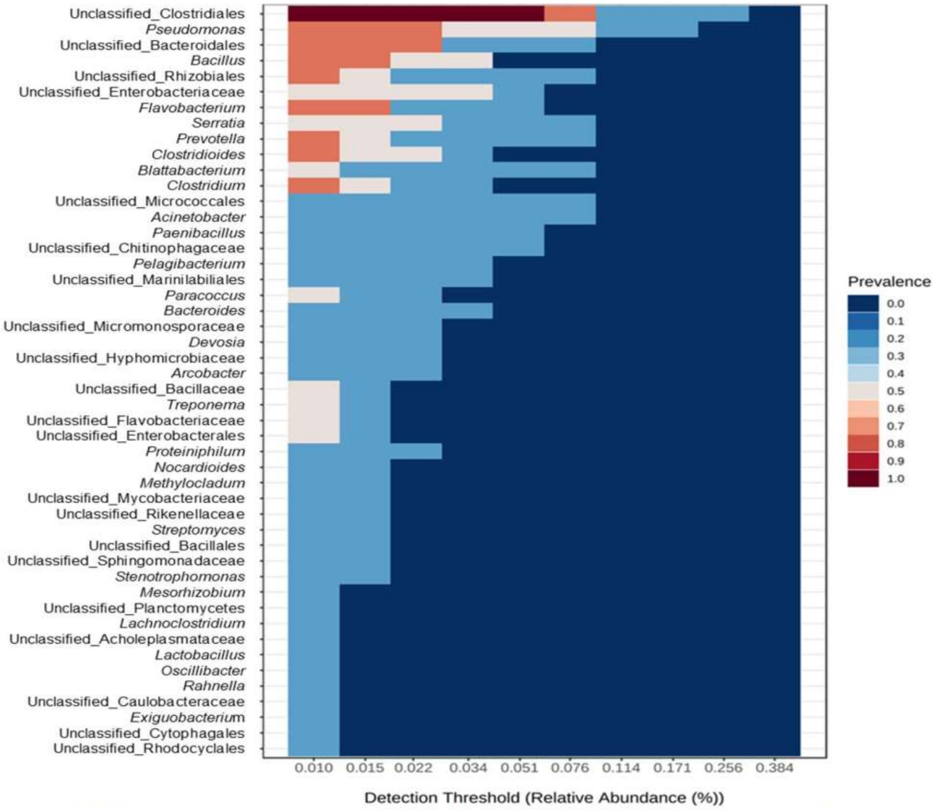

Figure 4.8. Heatmap representing the shared microbial genera within the core microbiomes

The Venn diagram is displayed in *Figure 4.9.* shared OTUs among initial and mature compost. Notably, 70 OTUs are common to both ADS and ADSRS, 5 overlap between ADSRS and CD, and 49 are shared across ADS, ADSRS, and CD. Ten are shared between ADS and CD. Three OTUs overlap in ADSRS, CD, and CDRS. The most extensive overlap comprises 178 OTUs among all four conditions. Six OTUs are common between ADS, CD, and CDRS. Thirty OTUs overlap between ADSRS and CDRS, while 91 are shared among ADS, ADSRS, and CDRS. Lastly, 12 OTUs are common to both ADS and CDRS. A comparative examination of distinct and overlapping operational taxonomic units (OTUs) uncovered distinct microbial profiles and collaborative relationships within composting processes, as shown in *Figure 4.9.*, fostering the decomposition of organic substrates [73].

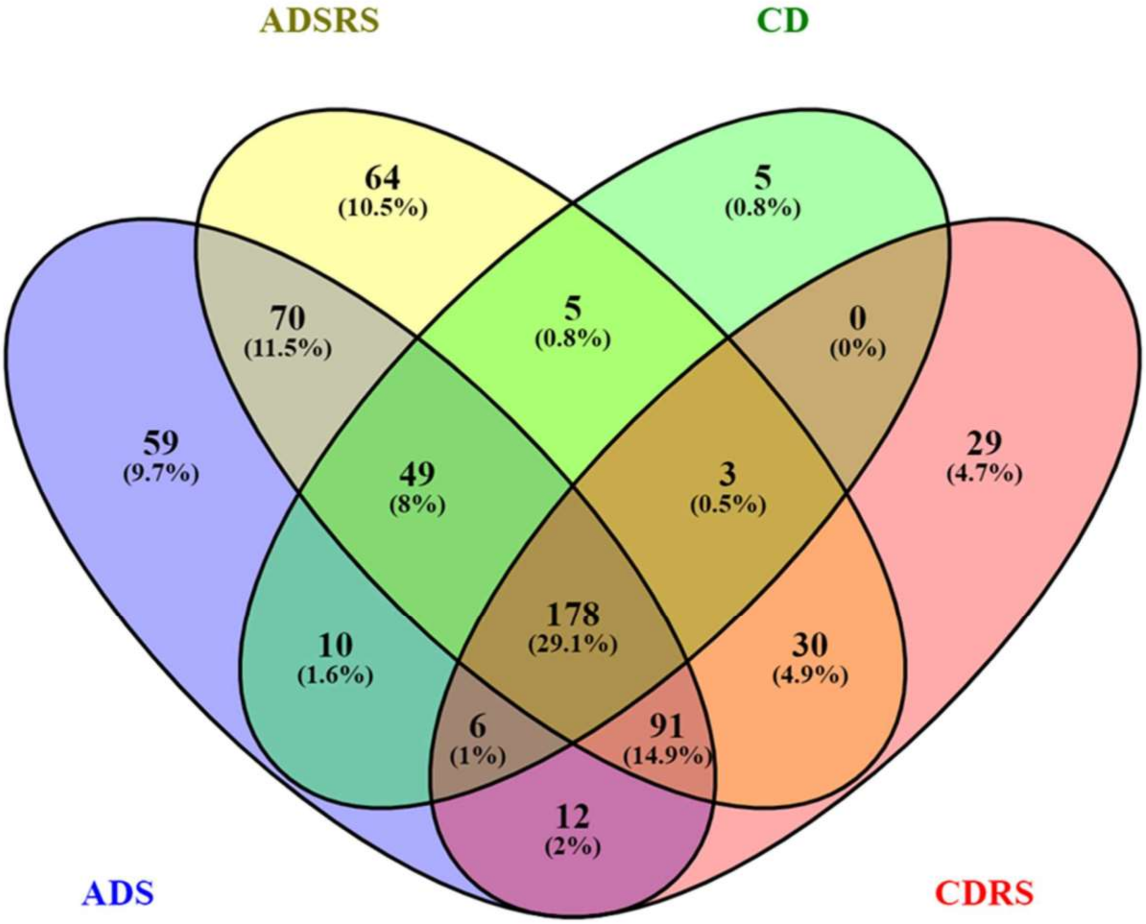

Figure 4.9. Venn diagram showing the distribution of shared bacterial OTUs among the four samples: ADS and CD (day 0), and ADSRS and CDRS (day 60)

The rarefaction curves depict species richness across various samples, as shown in *Figure 4.10*. Species richness increased in ADSRS compared to ADS, CD, and CDRS, while it decreased in CDRS compared to CD.

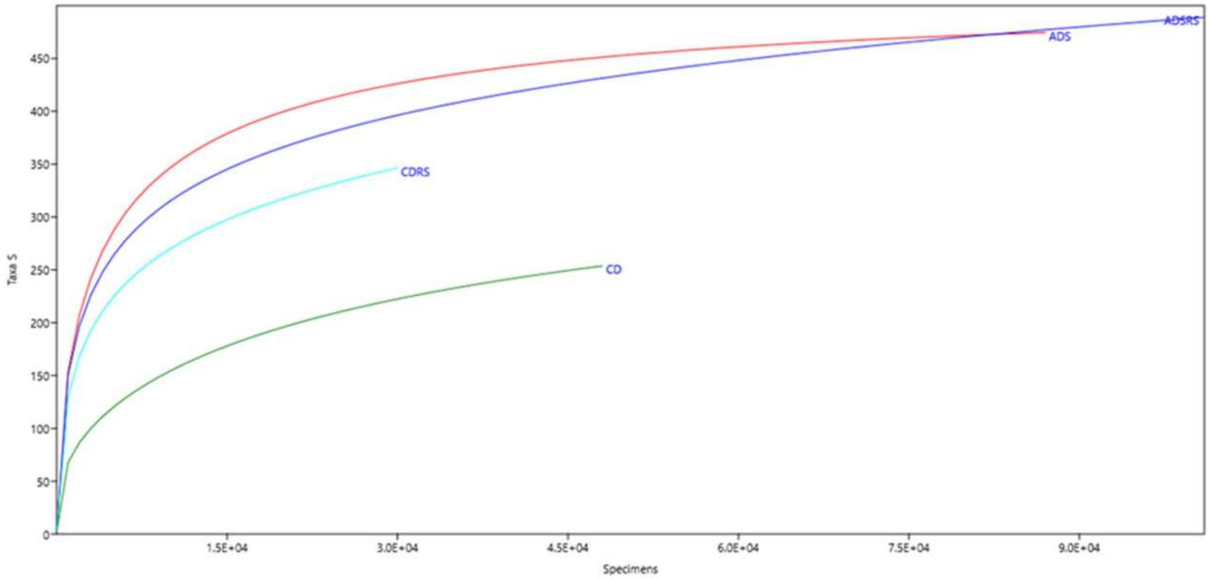

Figure 4.10. Rarefaction curve for initial (ADS and CD) and mature compost (ADSRS and CDRS)

4.2.5.2 Alpha diversity

Alpha diversity measures the richness and relative abundance of bacteria in a sample [91]. Table 4.2. displays various indices that represent measures of alpha diversity. The Chao 1 estimated species richness, reflecting each sample's total number of distinct species. Higher Chao 1 values indicated greater estimated species richness. Among the samples, ADSRS (390.27) exhibited the highest Chao 1 value, followed by ADS (372.48), CDRS (290), and CD (214.66), suggesting that ADSRS possibly contained the highest diversity of microbial species. The Fisher index assessed diversity and evenness within each sample. Elevated Fisher values indicated a more even distribution of species abundance. The ADS (57.52) and ADSRS (55.82) samples displayed relatively higher Fisher index values compared to CD (26.94) and CDRS

(41.91), implying a more balanced representation of different microbial species in ADS and ADSRS. The Shannon diversity index integrated species richness and evenness. Higher Shannon values indicated increased diversity. In line with the Chao 1 results, ADSRS (4.15) demonstrated the highest Shannon value, followed by ADS (3.82), CDRS (3.99), and CD (2.62), suggesting that ADSRS might have exhibited the most diverse and evenly distributed microbial community involved in composting. The Simpson diversity index illustrated dominance in each sample. Lower Simpson values indicated greater diversity. The Simpson index findings corresponded with other diversity indices, indicating that ADS (0.93) and ADSRS (0.96) possessed higher diversity compared to CD (0.82) and CDRS (0.96). The number of reads provided insight into sequencing depth and available genetic information for analysis. Higher read counts generally afforded a more accurate understanding of microbial diversity and community structure in composting. Among the samples, ADSRS (102162) recorded the highest read count, followed by ADS (88249), CD (49733), and CDRS (31144), indicating a greater depth of genetic information available for analysis in ADSRS.

Table 4.2. Comparison of alpha diversity measures in samples

Sample	Chao 1	Fisher	Shannon	Simpson	Number of reads
ADS	372.48	57.52	3.82	0.93	88249
ADSRS	390.27	55.82	4.15	0.96	102162
CD	214.66	26.94	2.62	0.82	49733
CDRS	290.00	41.91	3.99	0.96	31144

The ADSRS sample demonstrated the highest estimated species richness (Chao 1), diversity (Shannon index), and evenness (Fisher index). ADS and ADSRS exhibited greater diversity than CD and CDRS based on the Simpson index. Additionally, ADSRS showcased the highest number of reads, providing a deeper wealth of genetic information for analyzing its microbial community.

4.2.6 RDA analysis of flow cytometry populations and physicochemical parameters

Figure 4.11. depicted the redundancy analysis (RDA) conducted on flow cytometric data of microbial populations, recorded at ten-day intervals, in conjunction with various physicochemical compost parameters: temperature, pH, moisture, EC, nitrate, phosphate, TVFA, C/N ratio, carbon percentage, and nitrogen percentage. RDA synthesized variations in response variables utilizing computed explanatory variables [92]. Flow cytometry, a cost-effective, rapid, automated, and high-throughput technique, involved convenient sample preparation in small volumes and facilitated real-time integration. Flow cytometry data generated distinct fingerprints that enabled the investigation of patterns and dynamics within microbial populations. Changes in microbial dynamics were monitored to assess composter health rapidly. In *Figure 4.10.*, RDA ordination explained 77.70% (RDA 1) and 18.26% (RDA 2) of total distribution variability. Virtually all physicochemical explanatory variables exhibited positive correlations with microbial populations. Notably, CDRS40 and ADSRS40 correlated, possibly due to similar microbial dynamics linked to physicochemical properties. Flow cytometry data revealed positive correlations among populations 2, 3, 5, 6, and 7, with similarities between populations 3, 7, and 8. A distinct dissimilarity emerged between population 1 and population 2.

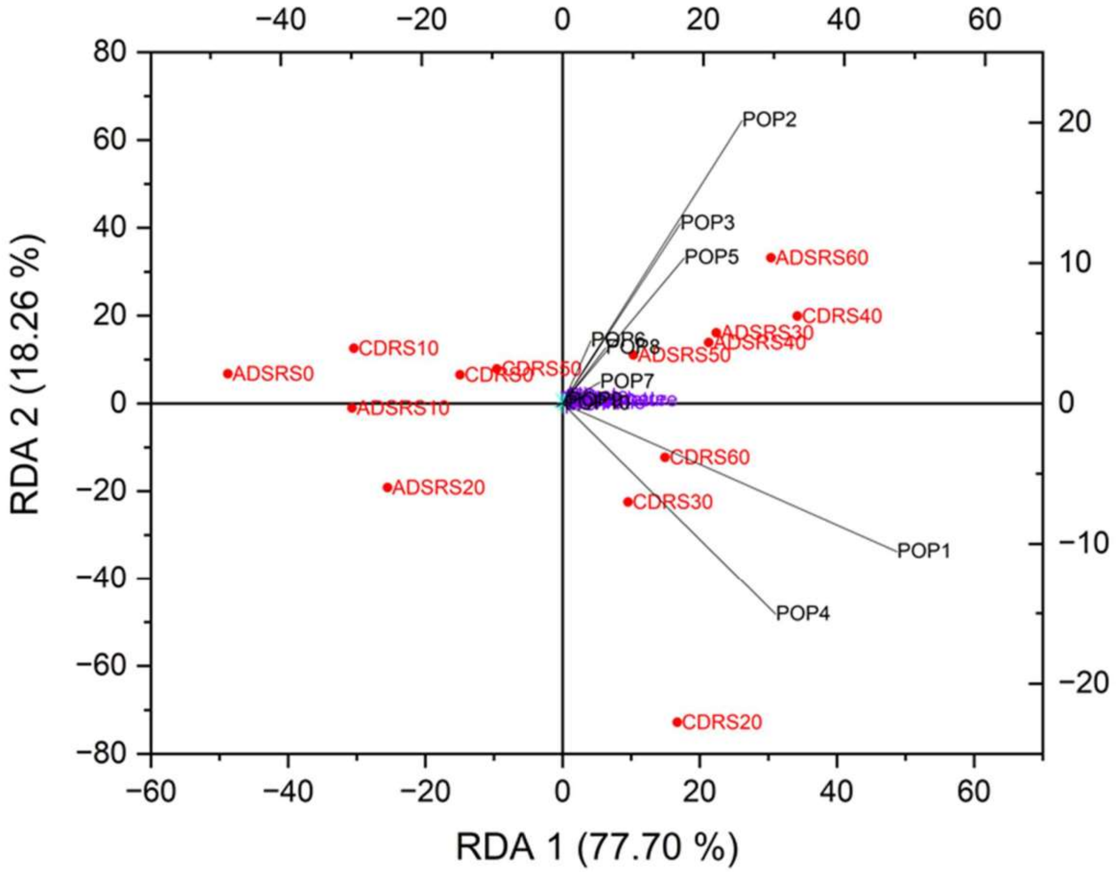

Figure 4.11. RDA analysis correlating flow cytometry microbial populations and physicochemical parameters

4.3 Limitations and future recommendations

Composting is pivotal in transforming agricultural residues, alleviating landfill pressures, and reducing methane release inherent in conventional straw disposal methods. The study's emphasis on digestate slurry as a potent inoculum source for RS composting highlights compost's essential role in sustainable waste management. However, the resilience of lignocellulosic biomass, prolonged digestion, and inadequate digestate handling impede efficient conversion. Costly pre-treatment methods further elevate overall production expenses. Nevertheless, the selection of suitable inoculum streamlines operations, irrespective of scale. Microbial genera within digestate slurry, such as *Prevotella, Acinetobacter, Bacillus, Serratia, Flavobacterium, Pseudomonas, Bacteroides, Clostridium, Proteiniphilum, Stenotrophomonas,* *Blattabacterium, Treponema, Clostridioides,* and *Paracoccus,* actively participate in composting. Collectively, they decompose diverse organic matter, contributing cellulose, starch, and protein-degrading enzymes that are crucial for nutrient cycling. Composting presents challenges in C:N ratio balancing, moisture control, and nutrient alignment, impacting microbial activity and final compost quality. Challenges such as surviving pathogens, temperature control, odor, and emissions further complicate the process. Managing these challenges requires meticulous adjustments in feedstock, moisture, nutrients, sanitation, and odor control for safe, high-quality compost production. Additionally, the combined use of RS and digestate slurry in composting provides a holistic approach to resource utilization, addressing agricultural residue management challenges while harnessing material synergy. This integrated approach not only mitigates environmental hazards linked to land dumping but also diminishes greenhouse gas emissions. Future prospects lie in optimizing composting processes, exploring innovative technologies for scalability, and integrating these practices into agricultural systems to advance circular economies, ensuring environmental conservation and food security amidst evolving agricultural landscapes. These initiatives could lay the foundation for the widespread adoption of composting in managing crop residues at a larger scale.

4.4 Conclusion

ADS and CD have exhibited their effectiveness as suitable sources of inoculum for RS composting. It is worth noting that ADS displayed a superior richness in microbial genera and phyla compared to CD. The observed increases in nitrate and phosphate concentrations, along with other physicochemical characteristics on particular days, further emphasize the crucial role of the core microbiome in facilitating compost maturation. The microbial community, consisting of genera like *Pseudomonas, Serratia, Prevotella, Flavobacterium, Acinetobacter, Bacillus, Streptomyces,* and *Chitinophagaceae,* alongside dominant phyla such as

Proteobacteria, Firmicutes, Bacteroidetes, and *Actinobacteria,* made substantial contributions to the improved degradation of RS. These insightful findings present a promising and sustainable avenue for addressing the challenges associated with RS management, while also showcasing the potential of ADS utilization.